

# Maximum entropy principle underlies wiring length distribution in brain networks

Yuru Song<sup>1</sup>, Douglas Zhou<sup>2,\*</sup>, Songting Li<sup>2,†</sup>

**1** School of the Gifted Young, University of Science and Technology of China, Hefei, Anhui, China

**2** School of Mathematical Sciences, MOE-LSC, and Institute of Natural Sciences, Shanghai Jiao Tong University, Shanghai, China

\*zdz@sjtu.edu.cn

†songting@sjtu.edu.cn

## Abstract

A brain network in general comprises a substantial amount of short range connections with an admixture of long range connections. Despite this common feature, the portion of long range connections between neurons or brain areas are observed to be quantitatively dissimilar for different species. It is hypothesized that the length of connections is constrained by the spatial embedding of brain networks, yet fundamental principles that underlie the wiring length distribution remain to be elucidated. By quantifying the structural diversity of a brain network using the measure of Shannon's entropy, here we show that the wiring length distributions across multiple species—including *C. elegans*, *Drosophila*, mouse, macaque, and human—share the feature of large entropy. Furthermore, these distributions can be well predicted by maximizing the entropy of wiring length under the constraints of limited wiring material and the spatial locations of neurons or brain areas. In addition, by taking into account stochastic axonal growth, we propose a network formation process capable of reproducing wiring length distributions of the five species as measured in experiments, thereby implementing the maximum entropy principle in a biologically plausible manner. We further develop a generative model incorporating the maximum entropy principle,

and show that, for the five species, the network reconstructed by the generative model exhibits higher similarity to the real network compared with those reconstructed by alternative models without accounting for network entropy. Our work suggests that the connectivity of brain networks evolves to be structurally diversified with large entropy to support its complex functions such as efficient inter-areal communication, thus provides a potential organizational principle of spatially embedded brain networks.

## Introduction

The dynamics of a brain network is substantially affected by its comprehensive connections. For instance, it has been shown that the functional connectivity recovered from resting-state cortical dynamics largely overlaps with the structural connectivity [1, 2]. In addition, cortical wave dynamics are often observed in the brain [3, 4]. Theoretical studies indicate that these waves originate preferably from hub areas in the network [5], and the emergence of the waves is influenced by the topology and connection distance of the network [6]. The topological structure of the brain network also highly correlates with the spatial gradients of specific brain functions [7]. Consequently, pathological perturbations to the brain structure will result in various brain disorders, as reviewed in Ref. [8]. For instance, in contrast to healthy controls, schizophrenia patients have a reduced hierarchical structure and an increased connection distance in their anatomically connected network of multi-modal cortex [9]. It is hypothesized that childhood-onset schizophrenia is induced by the overpruning of short distance connections during the developmental stage [10].

To quantitatively characterize the structure of brain networks, tools from graph theory and network science have been introduced into the neuroscience field [11, 12]. Following the conventions of network science terminology, neurons or brain regions are often described as nodes and the connections between them are described as edges.

Subsequently, network measurements including node degree distributions, clustering coefficients, path lengths, assortativity, and modularity have been calculated based on experimental measurements. It has been found that brain networks exhibit features of complex networks with highly connected hubs [13, 14] and modularity [14–16]. These network features are believed to facilitate functional integration and segregation of distinct brain regions [17–19]. In addition, brain networks have been identified with the small-world property characterized by small shortest path lengths and high clustering coefficients [20–22], which presumably maximizes the complexity of brain functions meanwhile saving wiring costs [21].

In addition to the aforementioned rich topological features, brain networks also possess the geometrical feature of spatial embedding [23]. This imposes constraints on the network structure [24, 25]. In fact, the network formation during brain development is largely determined by the gradients of growth factors across space [14]. As a consequence, neurons with similar functions tend to have more similar connection profiles than neurons with less similar functions [26, 27]. In addition, because brain networks are confined in a limited space, the number of neurons as well as the distance and cross-sectional diameter of axonal projections are substantially constrained by space [14]. Furthermore, the cost of establishing and maintaining axonal wiring connections increases with the wiring length of inter-neuronal connections [28]. To reduce wiring cost, a large number of connections in brain networks are observed to be local short connections [29, 30].

As a basic structural characteristic of brain networks, the distribution of wiring length has been measured in recent experiments. In general, the wiring length distribution is observed to peak at a short distance level and tail at a long distance level across multiple species [31, 32]. This fact indicates that brain networks comprise a substantial amount of short range connections with an admixture of long range

connections. The long range connections increase the wiring cost, and in return for this, they presumably bring important functional benefits such as supporting efficient communication [33] and facilitating functional diversity [32]. To further quantify the portion of long range connections, the shape of wiring length distribution has been statistically analyzed across species. In particular, the wiring probability as a function of distance between neurons in the neural network of *C. elegans* is best fitted by a power law distribution, and that in the neuronal network of rat visual cortex is best fitted by a Gaussian distribution [31]. In the inter-area network of macaque, the dependence of wiring probability on distance has been reported as gamma [31] and exponentially distributed [34] in two independent studies, respectively. Using scaling-theory, power-law distribution is theoretically proved to be the optimal solution of wiring length distribution under certain conditions [35].

Based on experimental observations, computational models have been developed to capture the distribution of wiring length. In particular, generative models have been proposed to well fit the wiring length distributions of macaque and human brain networks, respectively [34, 36, 37]. Yet these models often contain free parameters to be determined by fitting the network statistics. Accordingly, they are incapable of predicting the wiring length distribution without specifying the optimal parameter sets, thus impeding the understanding of the principle underlying the wiring length distribution. Alternatively, optimization models suggest that the wiring length distribution of the macaque brain network is optimally determined from the trade off between wiring cost and functional efficiency [38]. However, in contrast to the definition of wiring cost [28, 39], the definition of functional efficiency so far remains to be ambiguous. Therefore, the functional efficiency referred to as the shortest path length or others in the optimization models [38] is arguable [32, 36].

As a further step to understand the organizational principle of brain networks, the

following questions need to be addressed: (1) What is the common feature of the wiring length distributions across different species, if any? (2) Is there a fundamental principle underlying the wiring length distribution of a brain network? (3) How does the experimentally observed wiring length distribution emerge during network formation? (4) Are the experimentally observed wiring length distributions optimally designed for any brain function?

In this work, by quantifying the structural diversity of a brain network using the measure of Shannon’s entropy [38, 40, 41], we show that the wiring length distributions across multiple species—including *C. elegans*, *Drosophila*, mouse, macaque, and human—share the common feature of large entropy. Furthermore, these distributions can be well predicted by maximizing the entropy of wiring length under the constraints of (1) the spatial locations of neurons or brain areas and (2) the limited material resource described by average wiring length. This predictive framework is parameter-free as all the information required by the two constraints can be explicitly determined from experimental measurements. In addition, by considering stochastic axonal growth [31, 42], we propose a potential process of network formation to reproduce the wiring length distributions for multiple species as observed in experiments, thereby implementing the maximum entropy principle in a biologically plausible manner. We further develop a generative model incorporating the maximum entropy principle. For all the five species, We show that the network reconstructed by the generative model is more similar to the real network compared with those reconstructed by alternative models without accounting for network entropy. Finally, we discuss the functional implications of the maximum entropy principle, and show the predictability of the maximum entropy principle for other transport networks beyond brain networks including the flight network in the United States, the California road network, and the Shanghai subway network.

## Materials and methods

98

### Data source

99

We analyze the network structure of *C. elegans*, *Drosophila*, mouse, macaque, and human brain. In these networks, the connections are measured between neurons for *C. elegans*, while the connections are measured between brain areas for other species. In our analysis, we focus on the wiring length distribution of a network. Accordingly, we use the binary information of the network connectivity, i.e., the information of whether two areas or neurons are connected or not, although the network *per se* is directed and weighted. The data we analyze are obtained from the sites described below.

100

101

102

103

104

105

106

*C. elegans*. The network connectivity for *C. elegans* is reconstructed from two online databases (<https://www.wormatlas.org> and

107

108

<https://www.dynamic-connectome.org>). Both databases were based on the electron micrographs published in Ref. [43], and were updated with newly identified synapses.

109

110

The first database was provided and analyzed in Refs. [44–46], which incorporated additional synapses identified from other works [47,48]. The database includes 280

111

112

neurons, 6393 chemical synapses, 890 electrical junctions, and 1410 neuromuscular junctions. The chemical and electrical synapses are considered in our analysis. The

113

114

second database was published in Refs. [49,50], which includes 277 neurons and 2105

115

synapses. The database also includes the information of the two-dimensional spatial positions of neurons. The connectivity of the 277 neurons from these two databases do

116

117

not fully overlap with each other. In our analysis, we keep all the existing synapses in

118

the two databases, which yields 4758 connections between the 277 neurons in our

119

reconstructed network. This network is referred to as the *C. elegans* global network. We

120

use the information of the spatial positions of neurons provided by the second database.

121

In addition, we reconstruct a *C. elegans* local network composed of neurons in the

122

frontal area of the global network, which includes 169 neurons and 1331 connections.

123

The spatial layout of the global and local networks is shown in S1 Fig.

*Drosophila.* The network connectivity for *Drosophila* was reconstructed based on the data in Ref. [51], which is also available online in the FlyCircuit 1.2 database (<http://www.flycircuit.tw>). Labeled with green fluorescent protein, single neurons were imaged at high resolution, delineated from whole-brain three-dimensional images and co-registered to a *Drosophila* female adult template brain. The mesoscopic map was partitioned into 49 local processing units (LPU) with distinct morphological and functional characteristics. LPUs were defined so as to contain their own population of local interneurons whose fibers were limited to that specific LPU. We focus our analysis on the 2106 connections between the 49 LPUs.

*Mouse.* The network connectivity for mouse was reconstructed based on tract-tracing data in Ref. [52], which is also available on the Allen Institute Mouse Brain Connectivity Atlas (<http://connectivity.brain-map.org>). To build the database, axonal projections of neurons were traced with enhanced green fluorescent protein-expressing adeno-associated viral vectors, and imaged by high-throughput serial two-photon tomography throughout the brain. The viral tracer projection patterns were reconstructed and registered to a common three-dimensional reference space. Network areas were defined according to a custom parcellation based on the Allen Developing Mouse Brain Atlas. This parcellation contains 65 areas in each hemisphere, 9 of which were removed because they were not involved in any tract-tracing experiment. The resulting network contains 112 areas and 6542 connections.

*Macaque.* The network connectivity for macaque was reconstructed based on the online CoCoMac database (<http://cocomac.g-node.org/main/index.php>). The database covers connectivity data across literatures on tract-tracing experiments in macaque brain [53–56]. Later analysis of the database provides a direct repository of spatial positions of 95 cortical areas and 2390 connections between areas, which are

available on <https://www.dynamic-connectome.org> [49]. Recently, the database has been further improved and expanded to 103 cortical areas and 2518 connections using a more detailed parcellation of the motor regions [38, 57], which will be analyzed in our work.

*Human.* The human brain network we analyze is from Ref. [32], which includes 128 cortical areas and 4736 connections. It is reconstructed from diffusion weighted MRI, based on deterministic tractography algorithms. The data represents the composites of 30 human subjects.

## Generative models

We propose a generative model to demonstrate that the maximum entropy principle plays an important role in determining the brain network structure, in contrast to alternative models without considering network entropy.

The generative model is modified from Ref. [58] and is described as follows. In the model, the spatial locations of brain areas and their degree sequence are given from the real brain network we attempt to reconstruct, and the Euclidian distance between each pair of areas is calculated. To predict the network connectivity and statistics, we initialize the network by disconnecting all the areas, i.e., there is no connection in the initial network thus each area has a zero degree of connection. We then create a candidate list to include all the areas whose current degree is less than the target degree given by the degree sequence, and we put all the areas' ID into the candidate list initially. We next introduce an objective function  $F = H - \lambda * \bar{d}$  to help select a pair of areas to connect at each connection generating step, where  $H$  is the entropy of the network defined as  $H = -\sum_{i=1}^k p_i \log(p_i)$  and  $p_i$  is the probability of finding a connection with its length falling into the range  $[d_i, d_i + 1)$  in the current network,  $\bar{d}$  is the material cost or the average wiring length of the current network, and  $\lambda$  is a parameter that scales the relative contribution between network entropy and material



cost. The value of  $\lambda$  is chosen as 113 for *C. elegans* global network, 339 for *C. elegans* local network, 0.121 for *Drosophila* network, 0.791 for mouse network, 0.187 for macaque network, and 0.494 for human network, based on the optimal performance of network connectivity reconstruction of the generative model. In each step of connection generation, we utilize the greedy searching strategy: (1) For each area  $V_i$  in the candidate list, hypothetically connect it to another area  $V_j$  in the candidate list whose current degree has the largest difference from its target degree. (2) For each pair of  $V_i$  and  $V_j$ , compute the objective function  $F$  after adding the hypothetical connection between  $V_i$  and  $V_j$ . (3) Select the pair of  $V_i$  and  $V_j$  to connect which corresponds to the largest  $F$ . (4) Update the current degree of  $V_i$  and  $V_j$ , and update the candidate list if the degree of  $V_i$  or  $V_j$  reaches its target number. (5) Repeat the above steps until the candidate list becomes empty. We refer this model to as the MaxEnt-MinCost model.

In contrast, we further develop two alternative generative models for comparison as described below. In the first model, to remove the impact of the maximum entropy principle under the constraint of material cost on determining network structure, in each step of connection generation, we randomly choose a pair of areas to connect only under the constraint of degree sequence rather than based on optimizing  $F$ . This model is referred to as the fixed-degree model. The second model further removes the constraint of degree sequence. Accordingly, the network is reconstructed by randomly choosing a pair of areas to connect in each step until the total number of connections reaches that of the real brain network. This model is referred to as the random-degree model.

## Results

197

### Maximum entropy principle predicts the wiring length

198

#### distributions

199

The brain network in general consists of both short-range and long-range connections. It is evident that short-range connections can substantially save material cost. In contrast, long-range connections utilizes more material, which presumably benefits certain brain functions. However, the functional role of long-range connections remains to be fully elucidated, which impedes one to understand the spatial organization principle of the brain network. As the definition of network function remains arguable, here we investigate the organization principle from a different angle. Rather than exploring the functional benefits of network structure, we investigate the question of whether there exists any universal structural characteristic that brain networks evolve to possess, as whatever functional benefits are supported by network structure. We are particularly interested in the wiring length distribution of brain networks, which reveals the portion of short and long range connections that the brain invests resource to establish.

To address this question, we first analyze brain networks of four species — *Drosophila*, mouse, macaque, and human. The connections in these four networks are measured between brain areas (see Material and Methods for details). In addition, the wiring length  $d$  between two brain areas are measured by using the Euclidian distance, and all the wiring lengths are partitioned into even bins  $[d_i, d_{i+1})$ ,  $i = 1, 2, \dots, k$  to calculate the wiring length distribution  $p_i = P(d \in [d_i, d_{i+1}))$ . For the purpose of result demonstration, the number of bins is set to be  $k = 30$  for processing data obtained from different species, yet the results shown below are insensitive to the choice of bin number. As shown in Fig. 1, despite the fact that all the distributions of wiring length are unimodal, the shapes of these distributions are dissimilar. For instance, the wiring

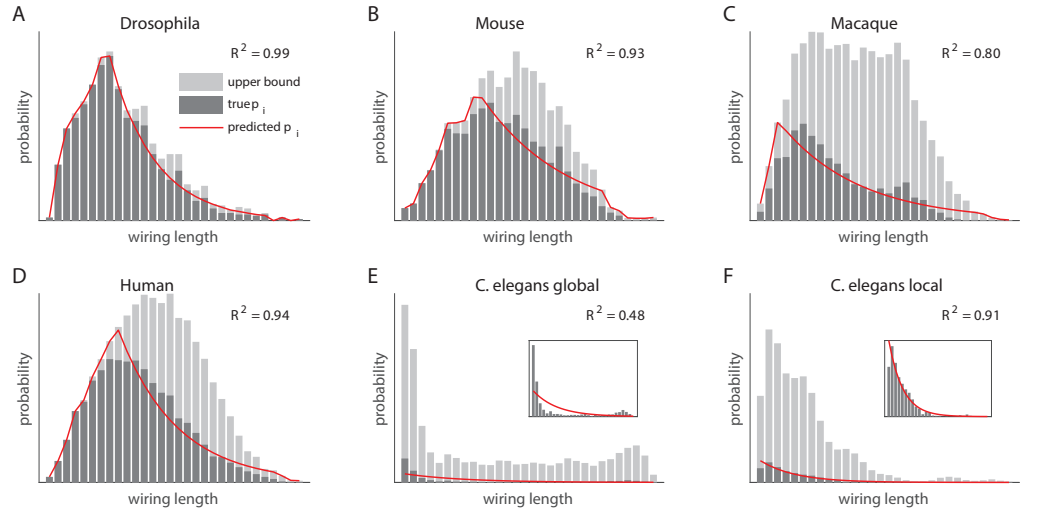


**Fig 1. Wiring length distributions of brain networks across multiple species and their predictions by the maximum entropy principle.** (A)-(D) are for brain networks of *Drosophila*, mouse, macaque, human, respectively. (E) and (F) are for the global and local neural networks of *C. elegans*, respectively. The insets of (E) and (F) are zooming in. In each panel, dark gray bars are the wiring length distribution measured from experiments. Silver bars are the upper bound of the wiring length distribution given by the reference distribution defined in the main text. Red solid line is the wiring length distribution predicted by the maximum entropy principle (Eqs. 1-4).  $R^2$  is calculated to evaluate the performance of the prediction. (A)-(F) share the same legend.

length distribution for macaque is heavily skewed, while that for human is nearly  
symmetric. The dissimilarity among the wiring length distributions for different species  
is caused by at least two factors, i.e., the spatial locations of brain areas as the  
constraint of space, and the total wiring length as the constraint of material cost.

To demonstrate the spatial constraints on a brain network, we first define the  
reference distribution as  $\frac{N}{M} \cdot q_i$ , where  $M$  is the number of connections in the real brain  
network,  $N$  is the number of connections in a corresponding fully connected brain  
network consisting of the same brain areas as the real brain network, and  $q_i$  is the  
wiring length distribution of the fully connected brain network. Note that the reference  
distribution is not a probability distribution as  $\sum_i \frac{N}{M} \cdot q_i = \frac{N}{M} \neq 1$ , yet the reference  
distribution gives the upper bound of  $p_i$ . As shown in Fig. 1, the wiring length  
distribution  $p_i$  is always under the reference distribution for all networks, i.e.,

$p_i \leq \frac{N}{M} \cdot q_i$ . This can be explained by the fact that the number of connections with  
wiring length falling into the bin  $[d_i, d_{i+1})$  shall be no larger than the number of all  
available connections with wiring length falling into the same bin, i.e.,  $p_i \cdot M \leq q_i \cdot N$ .  
In this sense,  $p_i$  is constrained by the spatial locations of brain areas.

In addition, for all the four networks, we note that the rising part of the wiring  
length distribution  $p_i$  nearly overlaps with the rising part of the reference distribution.  
Their overlap indicates that the brain network exploits almost all the short-range  
connections that are available to form. This observation supports the hypothesis that  
the brain network tends to form short-range connections in order to save material cost.  
Furthermore, as shown in Fig. 1, for all the four networks, the decay part of the wiring  
length distribution exhibits a substantial difference from their reference distribution.  
This observation suggests that the brain network chooses to form only a portion of  
long-range connections instead of all of the available ones, which presumably results  
from the constraint of wiring resource.

Note that the constraints of space and material are not sufficient to determine the  
wiring length distribution. In fact, under the two constraints, it remains feasible for the  
brain network to form additional long-range connections in compensation for removing  
short-range connections, and *vice versa*. Therefore, revealing the principle underlying  
the wiring length distribution is still an open question. It is hypothesized that the  
network structure is optimized for information processing functionally. However, the  
definition of functional efficiency of the brain remains ambiguous. Because the diverse  
function of the brain shall be supported by the network structure, we hypothesize that  
the network structure is optimally diversified through evolution.

Driven by this hypothesis, we introduce the measure of Shannon's entropy to  
quantify the diversity of the network structure. The entropy of a network is defined as  
 $H = -\sum_{i=1}^k p_i \log(p_i)$ , and is calculated for the four brain networks. As a reference, for

each brain network, we first construct one hundred random networks by randomly connecting each pair of brain areas until the total number of connections reaches that of the original brain network. The largest entropy value of these random networks approximates the upper bound of the brain network entropy. In addition, for each brain network, we construct a network with the smallest total wiring length while keeping the total number of connections identical to the original network. The entropy value of this network approximates the lower bound of the brain network entropy. Subsequently, we find that all the four brain networks possess large network entropy close to the upper bound while the network entropy is substantially larger than the lower bound, as shown in Fig. 2. The large entropy of these brain networks across different species attributes to their broad wiring length distributions, which indicates the large structural diversity of these networks.

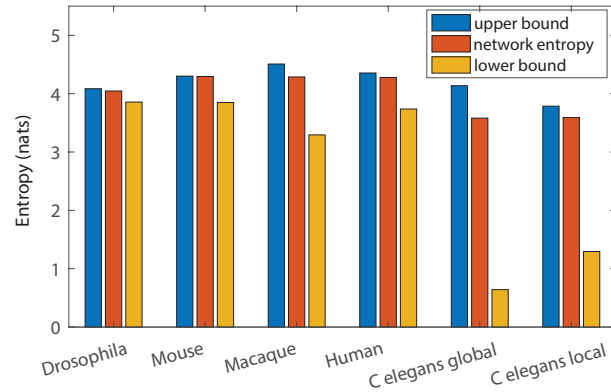


**Fig 2. Network entropy of the six brain networks.** Red bars correspond to the network entropy of *Drosophila*, mouse, macaque, human, the global and local networks of *C. elegans*. Blue and yellow bars are their upper and lower bounds respectively. See text for the calculation of the upper bound and lower bound of network entropy.

We next investigate the question of whether entropy maximization is sufficient to determine the wiring length distribution in addition to the constraints of space and material cost. We find that the wiring length distribution of all the four brain networks can be well predicted by the optimal solution of the following optimization problem,

$$\text{maximize} \quad -\sum_{i=1}^k p_i \log(p_i) \quad (1)$$

$$\text{subject to} \quad \sum_{i=1}^k p_i = 1 \quad (2)$$

$$\sum_{i=1}^k p_i \cdot d_i \leq \bar{d} \quad (3)$$

$$p_i \leq \frac{N}{M} q_i \quad \text{for } i = 1, 2, \dots, k \quad (4)$$

where Eq. 2 (probability constraint) is the normalization condition for probability  $p_i$ ; Eq. 3 (material constraint) requires the average wiring length to be no larger than an upper bound  $\bar{d}$ , which is measured as the average material cost in each brain network we aim to predict; Eq. 4 (space constraint) requires that the number of connections with wiring length in the range  $[d_i, d_{i+1})$  cannot exceed the number of all available connections with wiring length in the same range. It is noticed that this optimization problem (Eqs. 1-4) is parameter free.

We use CVX [59, 60] as a convex optimization problem solver to find the global optimal solution of Eqs. 1-4 for each of the four brain networks, i.e., *Drosophila*, mouse, macaque, and human brain. As shown in Fig. 1A-D, the optimal solutions well overlap with the experimentally observed wiring length distributions for all the four brain networks. Further,  $R^2$  is calculated to quantify the performance of the predictions— $R^2 = 0.99$  for *Drosophila* network,  $R^2 = 0.93$  for mouse network,  $R^2 = 0.80$  for macaque network, and  $R^2 = 0.94$  for human network.

In addition to analyzing the four brain networks with connections measured between brain regions, we have also analyzed the *C. elegans* network in which connections are measured between neurons. Fig. 2 shows that the network entropy of *C. elegans* also approaches to its upper bound while is substantially larger than its lower bound. In

addition, as shown in Fig. 1E, the prediction of the wiring length distribution from the maximum entropy principle fits the observed distribution moderately well with  $R^2 = 0.48$ . However, the performance of the prediction can be substantially improved in Fig. 1F with  $R^2 = 0.91$  by considering a local network located in the frontal area of the *C. elegans*. It is speculated that the moderate prediction performance of the *C. elegans* global network may attributes to the fact that the alignment of neurons in the global network is approximately one-dimensional. Such a network requires a large number of long-range connections for global information communication, which is underestimated by the wiring length distribution predicted by the maximum entropy principle.

We point out that the constraint of material cost in the optimization problem (Eqs. 1-4) is loosely set with an upper bound, which allows a network to use less material than the real one measured in experiment. This constraint together with the other two constraints allow a large feasible region of the optimization problem (Eqs. 1-4), i.e., there are a large number of possible solutions that satisfy the constraints. However, the objective function of entropy maximization picks out only one solution that is consistent with the wiring length distribution observed in the real brain network, indicating that entropy maximization can be a potential principle of brain network organization.

## Biological implementation of the maximum entropy principle

We next investigate biologically plausible implementation of the maximum entropy principle during the stage of network wiring formation. It has been found that neural wiring is determined by multiple factors, including gene expression [26,61], gradients of growth factors [14], randomness of axonal growth [31,42,62] and others. Here we hypothesize that stochastic axonal growth may play an important role in the implementation of the maximum entropy principle, as the concept of entropy in general characterizes the degree of randomness of a physical quantity.

Fig. 3A-C illustrates a process of network formation by stochastic axonal growth. In the growth model, the locations of all brain areas are embedded in the geometric space, and the distance between each pair of brain areas is set to be identical to that measured in experiment. Initially all brain areas are disconnected. A bunch of axons from each area start to grow out with a constant speed towards random directions in the three-dimensional space. The growth of an axon from one area terminates with certain probability once the axon reaches the vicinity of another area if that area has not been fully occupied. After sufficiently long simulation time, axons that fail to connect two areas will be pruned. To avoid the emergence of super rich hubs with unrealistically large number of degrees, each area is set to have a limited number of axons it can receive. In our simulations, the limited capacity for each area is set to equal the actual connection degree of the area. In addition, the radius of the “touching field” is chosen such that the total number of connections approximately equals that of the real brain network. Additional stochasticity is introduced by setting a failure probability of connection formation when an axon reaches the “touching field” of an area, which increases the chance of forming long-range connections. The values of these biological parameters, including the number of outgrowing axons per area, the speed of axonal growth, the radius of the “touching field”, and the failure probability of forming a new connection are listed in S1 Table. As shown in Fig. 3D-I, the random growth model well reproduces the wiring length distribution for all the brain networks across the five species, although the reproducing of the wiring length distribution for the *C. elegans* global network is moderately well. This result indicates that random axon growth may serve as a crucial factor that implements the maximum entropy principle.



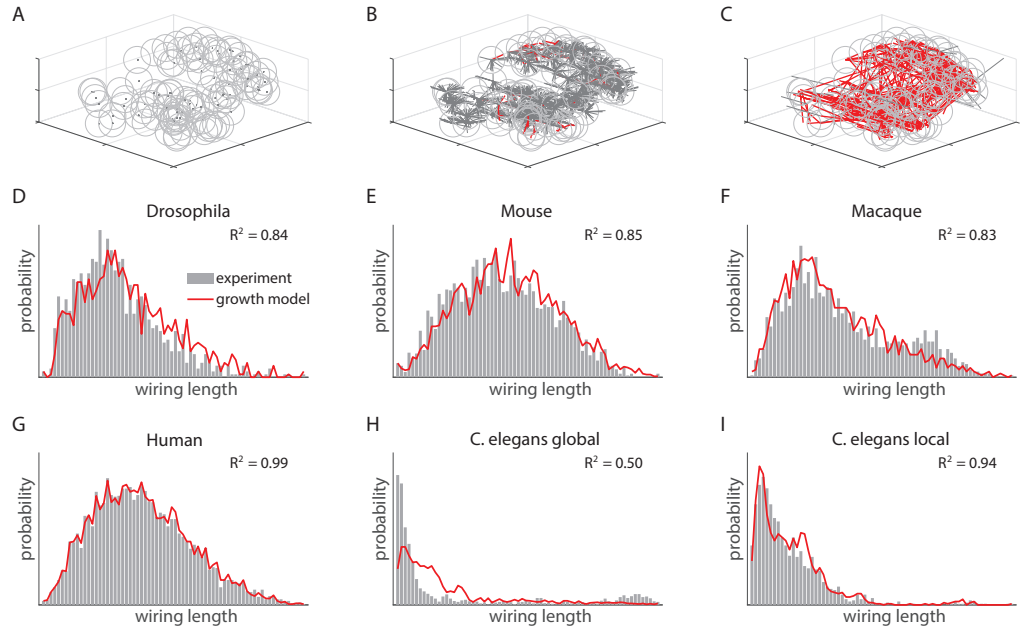


**Fig 3. Random axonal growth process reproduces the wiring length distributions of brain networks across multiple species.** (A)-(C), schematic illustration of the random growth process. (A), the initial state of a network with all areas disconnected. The locations of all the areas are based on experimental measurement. Gray circles are the “touching field” of each area. (B), the random growth stage of the network. A bunch of axons from each area start to grow out with a constant speed towards random directions. Connections are formed (red lines) with a certain probability when growing axons (black lines) fall into the touching field of another area. (C), the pruning state of the network. Networks are formed by finally pruning axons that fail to connect two areas. (D)-(I), the wiring length distributions of the brain networks for *Drosophila*, mouse, macaque, human, the global and local networks of *C. elegans*, respectively. The silver bars are from experimental measurement, and the red curves are from the simulations of stochastic axonal growth.

## Maximum entropy principle contributes to network connectivity and statistical properties

We further address the question of whether the principle of maximum entropy contributes to additional properties of network structure beyond the wiring length distribution, including network connectivity, clustering coefficient, and modular structure. The investigation of these network properties requires the recovery of network connections, which cannot be directly obtained from the wiring length distribution by solving the optimization problem (Eqs. 1-4).

To overcome this difficulty, we propose a generative model with the maximum entropy principle (Eqs. 1-4) incorporated (see model details in Materials and Methods). In brief, the generative model maximizes the quantity  $F = H - \lambda * \bar{d}$  at each connection generating step, where  $H$  is the entropy of the network,  $\bar{d}$  is the material cost or the average wiring length of the network, and  $\lambda$  is a parameter that scales the relative importance between network entropy and material cost. The process of connection generation stops until the connection degree of each area or neuron meets that measured in the real brain network. Note that the objective function  $F$  in the generative model takes the Lagrange Multiplier form of the optimization problem (Eq. 1) constrained by the material cost (Eq. 3), and the generative model naturally satisfies the constraints of probability normalization (Eq. 2) and space (Eq. 4). Therefore, the generative model optimizes network entropy constrained by material cost and space in each step of connection generation, thus solving Eqs. 1-4 effectively. We refer this model to as the MaxEnt-MinCost model. The MaxEnt-MinCost model provides more information than the solution of the optimization problem (Eqs. 1-4), i.e., the additional information of network connectivity thereafter statistical properties beyond the wiring length distribution. Therefore, the MaxEnt-MinCost model allows us to investigate the role of the maximum entropy principle in determining network structure and property.

Note that, in addition to incorporating the maximum entropy principle, the MaxEnt-MinCost model also incorporates the extra information of degree sequence, i.e., the degree of each area or neuron shall be identical to that measured in the real brain network. To substantiate the unique role of the maximum entropy principle on the determination of network structure, we further develop two alternative generative models for comparison (see model details in Materials and Methods). In the first model, in each step of connection generation, we randomly connect a pair of areas only under the constraint of degree sequence rather than optimizing  $F$ . The reconstructed network by this model has the same degree sequence as the real brain network. The model is referred to as the fixed-degree model. The fixed-degree model removes the influence of the maximum entropy principle on network structure while only accounts for the contribution of degree information to the determination of network structure. Accordingly, the improved performance from the fixed-degree model to the MaxEnt-MinCost model attributes to the maximum entropy principle. In addition, we propose a second generative model that further removes the information of degree sequence. This model is referred to as the random-degree model. Accordingly, the improved performance from the random-degree model to the fixed-degree model attributes to the additional information of degree sequence.

We first assess the performance of the generative models on the recovery of the network connectivity, which is evaluated by the recovery rate defined as the ratio of the number of successfully recovered connections by a generative model to the total number of existing connections in the real network. As shown in Fig. 4A, for the brain networks of *Drosophila*, Mouse, Macaque, and Human, the recovery rate of the MaxEnt-MinCost model is relatively high above 65%. In contrast, for the global and local networks of *C. elegans*, the recovery rate of the MaxEnt-MinCost model is as low as about 25%. The low recovery accuracy of the network connectivity for *C. elegans* is expected because of

its sparse network connection, which presents a great challenge for network  
reconstruction.

Fig. 4A shows that the recovered connectivity by the MaxEnt-MinCost model for all  
the five species is consistently and significantly more accurate than that of the  
random-degree model. This result indicates that network connectivity recovered by the  
MaxEnt-MinCost model is beyond random guess. Therefore, the network connectivity  
shall depend on the maximum entropy principle as well as degree sequence constraint as  
being considered in the MaxEnt-MinCost model. To demonstrate the relative  
contribution of the maximum entropy principle and the information of degree sequence  
in the MaxEnt-MinCost model to the recovery of network connectivity, the performance  
of the MaxEnt-MinCost model is compared with the fixed-degree model. The recovery  
rate drops from the MaxEnt-MinCost model to the fixed degree model due to the  
removal of the maximum entropy condition, indicating that the maximum entropy  
principle plays a unique role in determining network structure. The decrease of recovery  
rate from the MaxEnt-MinCost model to the fixed-degree model is about  $6.98\% \pm$   
 $4.76\%$  (mean  $\pm$  standard deviation for six networks across five species). In addition, the  
recovery rate further drops from the fixed-degree model to the random-degree model by  
 $8.02\% \pm 5.89\%$  in a consistent way for all the five species, demonstrating that degree  
sequence is also informative for the reconstruction of network connectivity.

We further show that maximizing network entropy in the MaxEnt-MinCost model  
also improves the recovery of network statistical properties including wiring length  
distribution, clustering coefficient, and modularity factor. We first investigate the  
performance of the generative models on recovering wiring length distribution evaluated  
by the Kolmogorov–Smirnov(K-S) statistic [63] [64]. By its definition, given a measured  
wiring length distribution and its prediction from one of the generative models, the  
smaller the K-S statistic value is, the closer the predicted wiring length distribution is

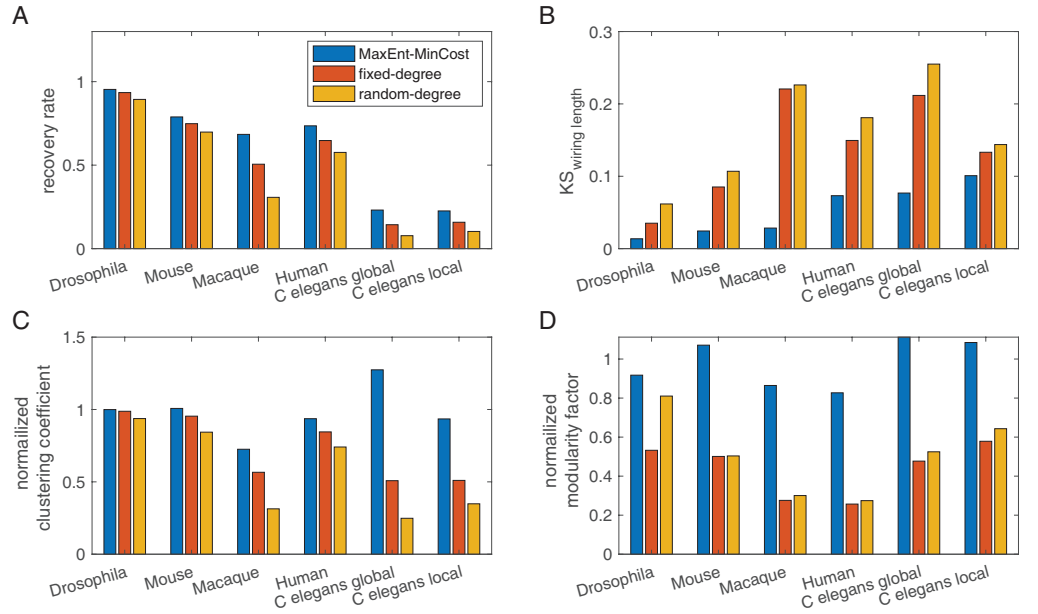


**Fig 4. Performance of the generative models on the prediction of network properties for the five species.** (A) recovery rate. (B) Kolmogorov–Smirnov statistic of the wiring length distribution measured in experiment and that recovered by the generative models. (C) Network clustering coefficient. (D) Network modularity factor. Data in (C) and (D) are normalized by dividing the real network’s clustering coefficient and modularity factors, respectively. (A)-(D) share the same legend in (A).

to the real distribution. Therefore, a smaller value of the K-S statistic indicates a better prediction from a generative model. As shown in Fig. 4B, among the three generative models, the MaxEnt-MinCost model best predicts the wiring length distribution of the brain networks for all the five species, and the performance drops by removing the constraint of the maximum entropy principle (i.e., the fixed-degree model), consistent with the previous result that the maximum entropy principle (Eqs. 1-4) well predicts the wiring length distributions. Similar hierarchy of model performance on the recovery of clustering coefficient [20] and modularity factor [65] of the brain networks are shown in Fig. 4C and Fig. 4D respectively. The MaxEnt-MinCost model that accounts for network entropy always outperforms the other two generative models without considering network entropy, particularly for the recovery of network modular structure. The successful recovery of the feature of network modularity by the MaxEnt-MinCost model is further demonstrated in Fig. 5, which clearly shows the effectiveness of the

MaxEnt-MinCost model in contrast to the fixed-degree model and the random-degree  
model.

## Functional implications of the maximum entropy principle

It is generally believed that the structure of a brain network supports its functional  
efficiency. We have shown that the structure of brain networks across various species  
share the common feature of large entropy or structural diversity, however, the  
functional benefit of structural diversity remains unclear. Previous works suggest that  
the efficiency of brain information processing can be possibly evaluated by the  
communication speed, i.e., the time it takes a neuronal signal to transmit from one area  
to another area [14]. One way to estimate the communication speed is to use the  
average shortest path (ASP) of the network [20]. By using mathematical analysis, we  
will first show that large structural diversity indeed corresponds to small ASP in an  
idealized brain network in which areas are evenly spaced in a ring. In addition, we will  
further show that the strong correlation between structural diversity and ASP can also  
be observed in four out of the six real brain networks measured in experiments.  
Therefore, a possible functional implication of structural diversity is to benefit  
information transmission in certain brain networks.

We first build an idealized brain network based on Ref. [66], in which ASP has been  
analytically calculated. As shown in Fig. 6A, in the idealized network, we consider  $L$   
brain areas located evenly in a ring lattice. Each area connects to its nearest  $2k$   
neighboring areas. In addition, a certain number of long-range shortcuts are added to  
the network to connect pairs of areas chosen randomly. The number of shortcuts are  
determined by the probability  $\phi$  per connection on the underlying ring lattice such that  
the total number of shortcuts is  $Lk\phi$  on average. By introducing a characteristic length  
parameter  $\xi = 1/(k\phi)$ , the average number of shortcuts becomes  $L/\xi$ , and the value of

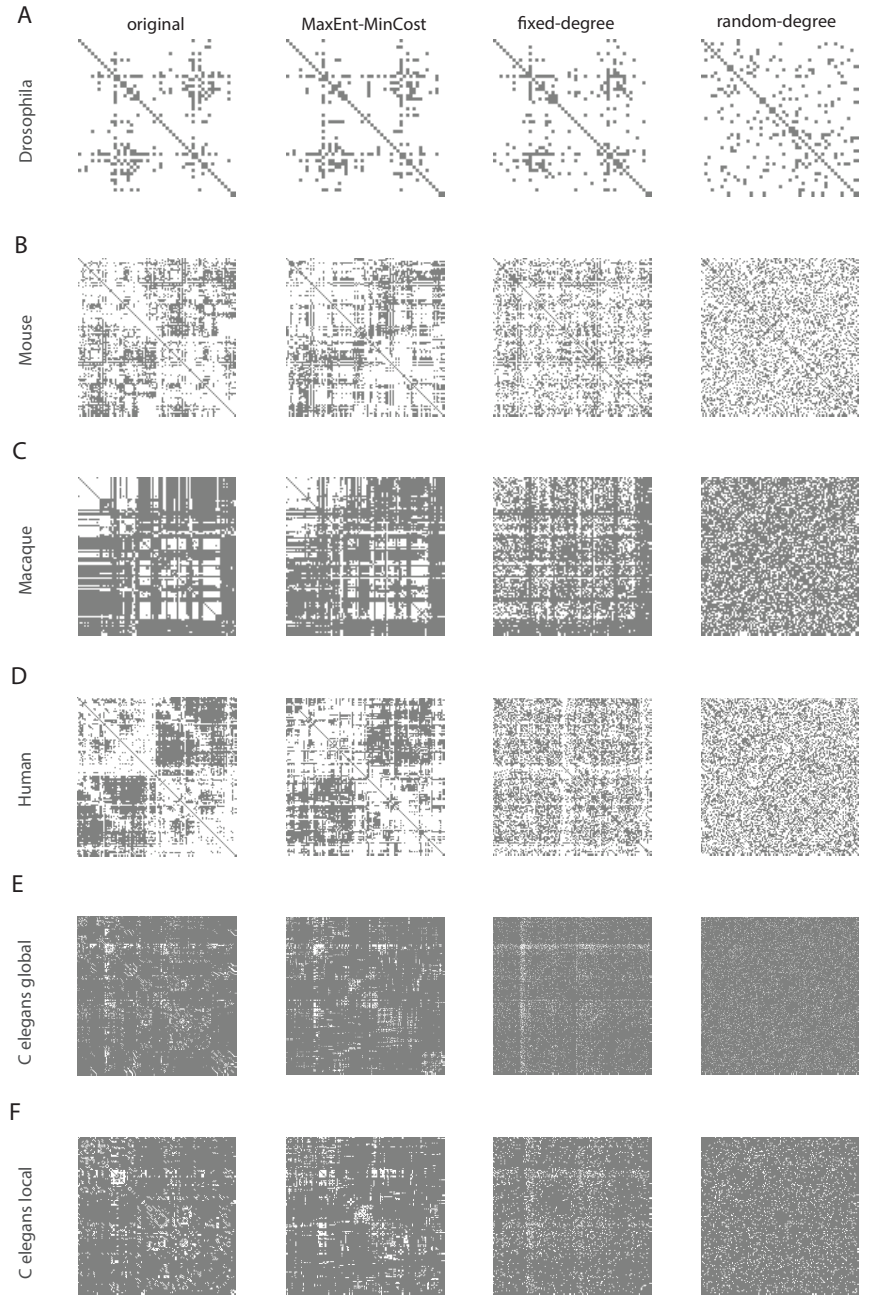


**Fig 5. Reconstruction of network connectivity from the generative models.** (A), *Drosophila* network. (B), mouse network. (C), macaque network. (D), human network. (E), global network of *C. elegans*. (F), local network of *C. elegans*. In each panel, the connectivity matrices recovered from the MaxEnt-MinCost model, the fixed-degree model, and the random-degree model are compared with the connectivity matrix of the real brain network. The MaxEnt-MinCost model well recovers the modular structure of the real network, while other models fail to recover it.

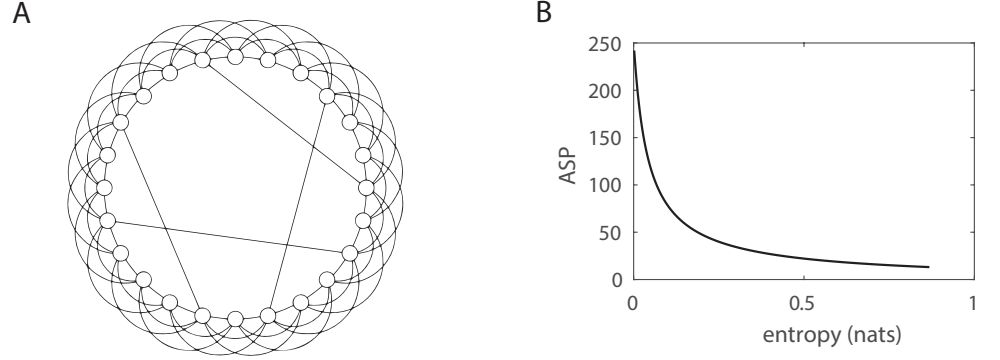


**Fig 6. Negative correlation between network entropy and ASP revealed in an idealized brain network.** (A), a schematic graph of an idealized brain network with 24 areas and 4 shortcuts. Each area connects to its nearest 6 neighboring areas. (B), ASP negatively correlates with network entropy derived from the mathematical analysis. The network has 1000 areas and each area connects to its nearest 2 neighbors.

ASP can be calculated as [66]

$$ASP = \frac{\xi}{2k\sqrt{1+2\xi/L}} \tanh^{-1} \frac{1}{\sqrt{1+2\xi/L}}.$$

To calculate the entropy of the network, we first describe the spatial location of each area in the ring network by an angular coordinate  $2\pi i/L$ , ( $i = 1, 2, \dots, L$ ). Subsequently, the distance between the  $i$ -th and  $j$ -th areas can be calculated as  $2\pi|i - j|/L$  in the angular space. To simplify the calculation, we assume  $L$  is an even number, thus the smallest and largest wiring lengths are  $2\pi/L$  and  $\pi$  respectively. We then discretize the wiring length distribution by dividing the distance range into  $L/2$  bins evenly, which are  $[\frac{3\pi}{2L}, \frac{5\pi}{2L}), [\frac{5\pi}{2L}, \frac{7\pi}{2L}), \dots, [\pi - \frac{\pi}{2L}, \pi + \frac{\pi}{2L})$ . If the probability  $\phi$  for adding a shortcut is zero, there are only  $L$  links belonging to each of the first  $k$  bins and there is no link in the remaining bins. Whereas if  $\phi$  is nonzero, an average number of  $Lk\phi$  shortcuts will be randomly and independently added to the network, hence the lengths of those shortcuts will fall into all the  $L/2$  bins with equal probability. Therefore, the number of shortcuts in each of the  $L/2$  bins is  $2k\phi$  on average. Accordingly, the connection length distribution is approximately



$$P(d \in i\text{th bin}) = \begin{cases} \frac{L}{kL + (L/2 - k)2k\phi} & \text{for } i \leq k \\ \frac{2k\phi}{kL + (L/2 - k)2k\phi} & \text{for } i > k \end{cases}$$

based on which we can calculate the network entropy as

$$H = -\frac{kL\xi}{kL\xi + L - 2k} \ln(L\xi) - \frac{L - 2k}{kL\xi + L - 2k} \ln(2) + \ln(kL\xi + L - 2k).$$

As shown in Fig. 6B, as the parameter  $\phi$  increases, the network entropy increases while the ASP decreases. Therefore, large entropy in this idealized brain network corresponds to small ASP of the network, which supports fast communications between brain areas. Note that by increasing  $\phi$ , the idealized network evolves from regular-lattice network towards small-world network. The latter possesses the features of high clustering coefficient and short ASP, which are similar to those observed in real brain networks. Therefore, the functional implication of large entropy for supporting efficient communications in the idealized network may also be valid in some brain networks.

We next examine the data of real brain networks to further verify the hypothesis that large entropy or structural diversity correlates with small ASP. It is noticed that the real brain network deviates from the idealized case mentioned above in that the layout of the brain areas or neurons are not spatially uniform. Therefore, for each brain network of the five species, we first construct a corresponding approximately “spatially-regular” network by having each area connecting with a fixed number of spatially nearest neighboring areas. The number of connections is approximately identical for each area and is determined by the way such that the total number of connections in the spatially-regular network is the same as the real brain network. Because most connection lengths are short, the wiring length distribution of this network is narrowly peaked. Accordingly, the network entropy is small. We label the false positive (FP)

connections and false negative (FN) connections in the spatially-regular network by  
comparing it with the real network. We then correct these connections step by step. In  
each step, we exchange a pair of connections from FP and FN pools which has the  
shortest length in the pools. Entropy and ASP are calculated throughout the correction  
steps. After a finite number of steps, the network will be corrected to the real network.  
As shown in Fig. 7, except for *Drosophila* and mouse, all the brain networks show the  
strong negative correlation between network entropy and ASP—the entropy increases  
while the ASP decreases as the correction continues, suggesting that the maximization  
of network entropy benefits communication efficiency in these networks.

In contrast, for the *Drosophila* and mouse networks, as they evolve from  
spatially-regular to the real one, network entropy increases while the ASP remains  
constant. The insensitivity of the ASP to network connectivity results from the fact  
that the two networks are densely connected, thus the ASP is small by all means in the  
presence of a large amount of connections. The two exception cases of the *Drosophila*  
and mouse networks indicate that the maximization of network entropy can be a more  
general principle than the minimization of ASP under the constraint of limited material  
resource, as has been hypothesized in previous works [38]. As shown in Fig. 7, for brain  
networks of *Drosophila* and mouse, the optimal network structure of both small ASP  
and small material cost shall be the spatially-regular network rather than the real  
network. In addition, for the human brain network, such an optimal network structure  
exists in the middle of the correction step. Therefore, these brain networks do not  
achieve the optimal balance between ASP and material costs. In these networks, large  
entropy may have other functional implications, for instance, enhancing functional  
diversity [32] or robustness [67] of the network. The diverse wiring length distribution  
may also provide a broad spectrum of conduction delays of action potential and support  
a rich pool of neural dynamics, which echoes the previous theoretical studies about the

temporal coding of spikes in the neural network [68]. All these speculations require future investigations.

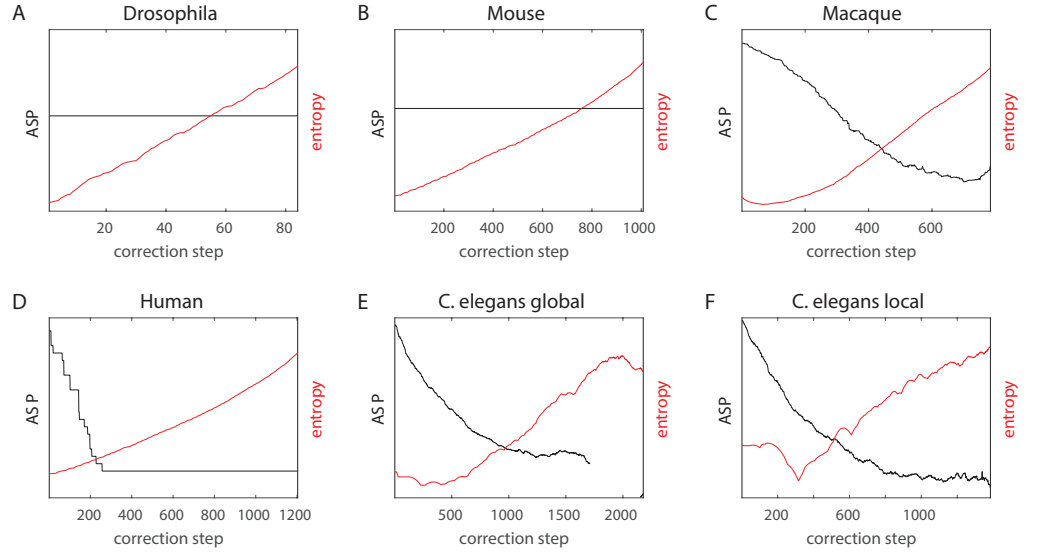


**Fig 7. Negative correlation between network entropy and ASP for brain networks of the five species.**(A), *Drosophila* network. (B), mouse network. (C) Macaque network. (D), human network. (E), global network of *C. elegans*. (F), local network of *C. elegans*.

## Discussion

In this work, we have shown that the wiring length distributions of brain networks across multiple species—including *C. elegans*, *Drosophila*, mouse, macaque, and human—share the feature of large entropy. These distributions have been well predicted by maximizing the entropy of wiring length under the constraints of limited wiring material and the spatial locations of neurons or brain areas. In addition, we have proposed a process of random axonal growth to reproduce wiring length distributions for the species as measured in experiments, thereby implementing the maximum entropy principle in a biologically plausible manner. We have further developed a generative model incorporating the maximum entropy principle, i.e., the MaxEnt-MinCost model. We have shown that the MaxEnt-MinCost model significantly improves the recovery

rate and other network statistics compared with alternative models without accounting 531  
for entropy, confirming that entropy maximization involves in determining the structure 532  
of brain networks. Our work indicates that the connectivity in brain networks evolves to 533  
be structurally diversified to support its complex function such as efficient signal 534  
communications between brain areas. 535

Network functions in general are realized by its dynamics, which can be substantially 536  
influenced by network structure [69]. Motivated by this, in this work, we focus on the 537  
network structure *per se* and ask the question of what structural features the brain 538  
network optimally evolves to possess under certain spatial and structural constraints. 539  
We then discuss the functional implications of the network structure based on our 540  
observation of large network entropy across species. This distinguishes our work from 541  
previous works attempting to understand network structure from the viewpoint of 542  
functional benefits, which lacks a clear definition yet [33, 70–72]. 543

It is undeniable that, during the developmental stage of each individual organism, 544  
the formation of the macroscale structure of brain networks is largely determined by 545  
genetic factors rather than being random. The variability of macroscale brain 546  
connectivity across individuals are relatively small. Therefore, the random growth 547  
process we proposed shall lie in the evolutionary time scale in which natural selection 548  
may play a role in pruning the randomly shaped network structures. However, the 549  
random growth model may be valid during the formation of the microscale structure of 550  
neuronal networks within a local brain area, where randomness is involved during the 551  
developmental stage of an individual’s brain. 552

Although the focus of this work is on brain networks, the maximum entropy 553  
principle can be applied to other transport networks beyond brain networks. To 554  
demonstrate this, we have examined the networks of the Shanghai subway, the flight in 555  
the United States, and the California Road. As shown in S2-S4 Figs., under the 556

constraints of limited wiring material and the spatial locations of nodes, the wiring length distributions of these networks can also be well predicted by maximizing the entropy of wiring length. The diversity of network structures is supposed to benefit the efficiency of traffic transport in these networks.

In our work, we have also confirmed that material cost has a crucial impact on network structure [14]. This is demonstrated in the objective function in the MaxEnt-MinCost model  $F = H - \lambda \bar{d}$ , where  $H$  is the network entropy and  $\bar{d}$  is the average wiring length. The parameter  $\lambda$  scales the relative importance between the two quantities, and the optimal value of  $\lambda$  that leads to the most accurate network reconstruction is large in general, indicating the importance of the material cost in determine network connectivity. If we view  $\lambda$  as the cost per unit length, as the cost increases, network structure will change accordingly. For instance, as shown in Fig. 8, the networks reconstructed under various  $\lambda$  have distinct clustering coefficients. The larger the  $\lambda$  is, the more expensive the material cost is. As can be inferred from the black curve in Fig. 8, the clustering coefficient has an overall increase under larger material cost with exception at certain  $\lambda$  value. Interestingly, by aligning the best-performance  $\lambda$  value marked by the red dashed line with the experimentally identified network clustering coefficient marked by the red star, we find that the peaks of the clustering coefficient value across species lie around the best reach of our generative model. The most distinct peak can be observed in the *C. elegans* local network, implying other unidentified factors recruited in constructing the neural network and leading to even higher clustering coefficient with a moderate material cost. Although the *Drosophila* and mouse networks possess less evidence of this phenomenon, the recovery rates are already high.

Many algorithms have been proposed for reconstructing neural networks and have achieved good performances [37,38]. Yet it remains challenging to fully recover the

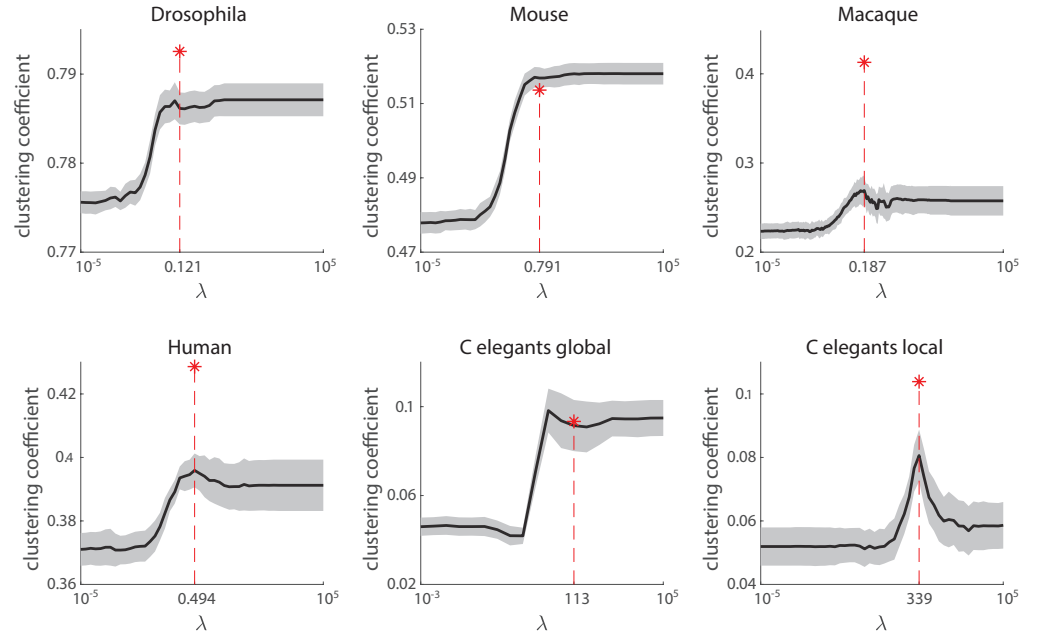


**Fig 8. The dependence of clustering coefficient on  $\lambda$  in the MaxEnt-MinCost model.** (A), *Drosophila* network. (B), mouse network. (C), macaque network. (D), human network. (E), global network of *C. elegans*. (F), local network of *C. elegans*. The black line is the average clustering coefficient. The shaded grey area as the standard deviation calculated from multiple trials of realization, whose number is the same with node number in the network. The red star shows the clustering coefficient value of the corresponding biological brain network. The vertical red dashed line together its value on the abscissa give the  $\lambda$  value for the best performance MaxEnt-MinCost generative network.

connectivity of a brain network. One challenge lies in the huge space of network configurations. In general, the reconstruction algorithms start with neurons or areas being disconnected. Connections are added gradually based on certain optimization rules. For a network of  $N$  nodes, the potential network configurations can be as many as  $N!$ , which is about  $10^{164}$  for the macaque cortical network. Therefore, exhaustive searching is impossible to realize. The MaxEnt-MinCost model partially solves the problem by achieving an accuracy of recovery rate 68% in macaque cortical network, which is comparable with earlier algorithms [37,38]. Another challenge lies in the identification of factors that determine network structure. The structure of brain networks is determined by various factors, for instance, spatial geometry, gene expression, gradients of growth factors, randomness of axonal growth, and budgets of

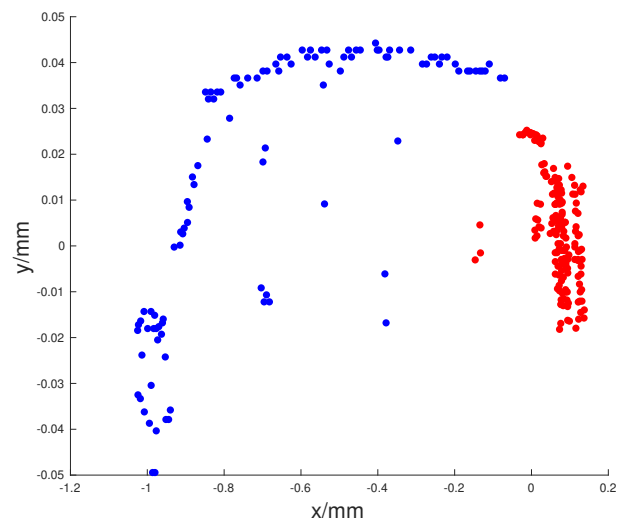
energy consumption and material cost. Here we have shown that the network statistics  
of wiring length distribution is largely determined by the spatial constraint and material  
cost constraint when maximizing network entropy, and realized by random axonal  
growth. However, these factors are insufficient to accurately recover network  
connectivity, as demonstrated by the performance of the MaxEnt-MinCost model.  
Therefore, to incorporate more factors in the generative model can be a future direction  
to understand network connectivity. In addition, the MaxEnt-MinCost model can be  
further modified by taking into account the direction and weight of connections in the  
future study.

## Acknowledgments

The authors thank Richard Betzel for sharing the data of the *Drosophila*, mouse, and  
human brain network, and thank Christopher J. Honey, Yuhua Chen, and Yanyang  
Xiao for helpful discussions. This work is supported by National Natural Science  
Foundation of China Grants 11901388, Shanghai Sailing Program 19YF1421400,  
Shanghai Chengguang program (S.L.), and Shanghai Rising-Star Program  
15QA1402600, Natural Science Foundation of China Grants 11671259, 11722107,  
91630208 (D.Z.), and by Student Innovation Center at Shanghai Jiao Tong University.

S1 Table. Parameters in the random growth model for the six brain networks.

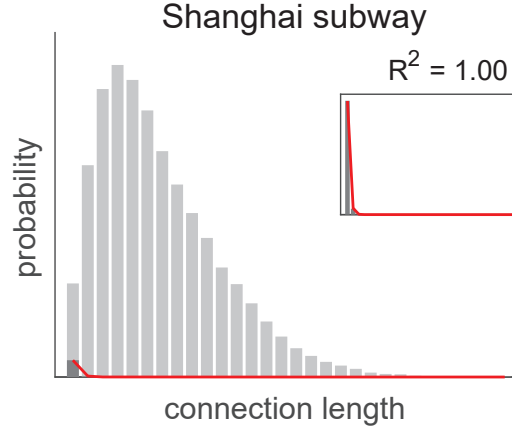
|                          | Number of outgrowing axons | Radius of touching area in unit of network size | Growth speed | Failure probability of synapse formation |
|--------------------------|----------------------------|---|--------------|--|
| <i>Drosophila</i>        | 200                        | 0.43  | 0.1          | 0.5                                      |
| Mouse                    | 200                        | 0.2   | 0.1          | 0.5                                      |
| Macaque                  | 200                        | 0.13  | 0.1          | 0.5                                      |
| Human                    | 200                        | 0.173   | 0.1          | 0.5                                      |
| <i>C. elegans</i> global | 50                         | 0.2   | 0.2          | 0.8                                      |
| <i>C. elegans</i> local  | 40                         | 0.2   | 0.2          | 0.965                                    |



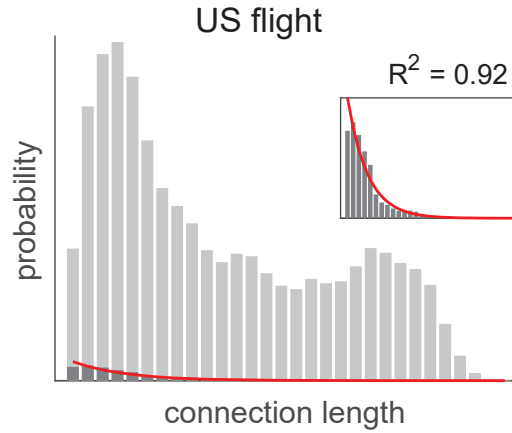
S1 Fig. The spatial layout of neurons in *C. elegans*. Each dot represents a neuron. Neurons marked by red compose the local network of *C. elegans*. The coordinates represent the locations of each neuron in the actual body in the unit of mm.

Supporting information

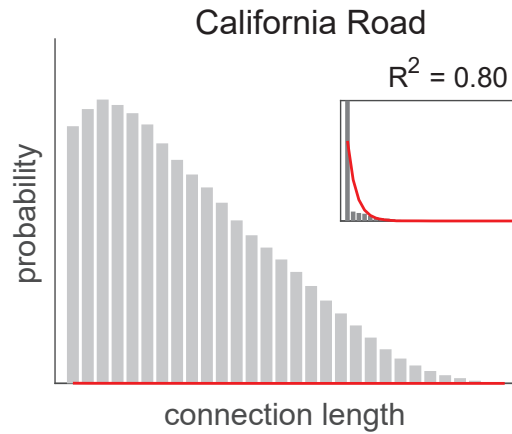




**S2 Fig. Wiring length distribution of the Shanghai subway network.** Dark gray bars are the wiring length distribution measured from the subway network. Silver bars are the upper bound of the wiring length distribution given by the reference distribution defined in the main text. Red solid line is the wiring length distribution predicted by the maximum entropy principle (Eqs. 1-4).  $R^2$  is calculated to evaluate the performance of the prediction. The data is downloaded from <http://www.shmetro.com>.



**S3 Fig. Wiring length distribution of the US flight network.** Dark gray bars are the wiring length distribution measured from the flight network. Silver bars are the upper bound of the wiring length distribution given by the reference distribution defined in the main text. Red solid line is the wiring length distribution predicted by the maximum entropy principle (Eqs. 1-4).  $R^2$  is calculated to evaluate the performance of the prediction. The data is available on <https://openflights.org/data.html>.



**S4 Fig. Wiring length distribution of the California road network.** Dark gray bars are the wiring length distribution measured from the California road network. Silver bars are the upper bound of the wiring length distribution given by the reference distribution defined in the main text. Red solid line is the wiring length distribution predicted by the maximum entropy principle (Eqs. 1-4).  $R^2$  is calculated to evaluate the performance of the prediction. The data is downloaded from <http://www.cs.utah.edu/~lifeifei/datasets.html>.

## References

1. Honey CJ, Kötter R, Breakspear M, Sporns O. Network structure of cerebral cortex shapes functional connectivity on multiple time scales. *Proceedings of the National Academy of Sciences*. 2007;104(24):10240–10245.
2. Zhou D, Xiao Y, Zhang Y, Xu Z, Cai D. Causal and structural connectivity of pulse-coupled nonlinear networks. *Physical review letters*. 2013;111(5):054102.
3. Rubino D, Robbins KA, Hatsopoulos NG. Propagating waves mediate information transfer in the motor cortex. *Nature neuroscience*. 2006;9(12):1549.
4. Muller L, Chavane F, Reynolds J, Sejnowski TJ. Cortical travelling waves: mechanisms and computational principles. *Nature Reviews Neuroscience*. 2018;19(5):255.
5. Roberts JA, Gollo LL, Abeysuriya RG, Roberts G, Mitchell PB, Woolrich MW, et al. Metastable brain waves. *Nature communications*. 2019;10(1):1056.
6. Jirsa VK, Haken H. Field theory of electromagnetic brain activity. *Physical Review Letters*. 1996;77(5):960.
7. Jbabdi S, Sotiropoulos SN, Behrens TE. The topographic connectome. *Current opinion in neurobiology*. 2013;23(2):207–215.
8. Fornito A, Zalesky A, Breakspear M. The connectomics of brain disorders. *Nature Reviews Neuroscience*. 2015;16(3):159.
9. Bassett DS, Bullmore E, Verchinski BA, Mattay VS, Weinberger DR, Meyer-Lindenberg A. Hierarchical organization of human cortical networks in health and schizophrenia. *Journal of Neuroscience*. 2008;28(37):9239–9248.
10. Feinberg I. Schizophrenia: caused by a fault in programmed synaptic elimination during adolescence? *Journal of psychiatric research*. 1983;17(4):319–334.

11. Bullmore E, Sporns O. Complex brain networks: graph theoretical analysis of structural and functional systems. *Nature reviews neuroscience*. 2009;10(3):186.
12. Bassett DS, Sporns O. Network neuroscience. *Nature neuroscience*. 2017;20(3):353.
13. van den Heuvel MP, Kahn RS, Goñi J, Sporns O. High-cost, high-capacity backbone for global brain communication. *Proceedings of the National Academy of Sciences*. 2012;109(28):11372–11377.
14. Bullmore E, Sporns O. The economy of brain network organization. *Nature Reviews Neuroscience*. 2012;13(5):336.
15. Meunier D, Lambiotte R, Bullmore ET. Modular and hierarchically modular organization of brain networks. *Frontiers in neuroscience*. 2010;4:200.
16. Sporns O, Betzel RF. Modular brain networks. *Annual review of psychology*. 2016;67:613–640.
17. Young MP. Objective analysis of the topological organization of the primate cortical visual system. *Nature*. 1992;358(6382):152.
18. Hilgetag CC, Burns GA, O’Neill MA, Scannell JW, Young MP. Anatomical connectivity defines the organization of clusters of cortical areas in the macaque and the cat. *Philosophical Transactions of the Royal Society of London Series B: Biological Sciences*. 2000;355(1393):91–110.
19. Hilgetag CC, Kaiser M. Clustered organization of cortical connectivity. *Neuroinformatics*. 2004;2(3):353–360.
20. Watts DJ, Strogatz SH. Collective dynamics of ‘small-world’ networks. *nature*. 1998;393(6684):440.
21. Bassett DS, Bullmore E. Small-world brain networks. *The neuroscientist*. 2006;12(6):512–523.
22. He Y, Chen ZJ, Evans AC. Small-world anatomical networks in the human brain revealed by cortical thickness from MRI. *Cerebral cortex*. 2007;17(10):2407–2419.
23. Barthélemy M. *Spatial networks*. Springer; 2018.
24. Ramon-y Cajal S, Swanson N, Swanson LW, Guillery R. Histology of the nervous system. *Trends in Neurosciences*. 1996;19(4):156–156.
25. Stiso J, Bassett DS. Spatial embedding imposes constraints on neuronal network architectures. *Trends in cognitive sciences*. 2018;.
26. French L, Pavlidis P. Relationships between gene expression and brain wiring in the adult rodent brain. *PLoS computational biology*. 2011;7(1):e1001049.
27. Rubinov M, Ypma RJ, Watson C, Bullmore ET. Wiring cost and topological participation of the mouse brain connectome. *Proceedings of the National Academy of Sciences*. 2015;112(32):10032–10037.
28. Chklovskii DB. Exact solution for the optimal neuronal layout problem. *Neural computation*. 2004;16(10):2067–2078.
29. Hellwig B. A quantitative analysis of the local connectivity between pyramidal neurons in layers 2/3 of the rat visual cortex. *Biological cybernetics*. 2000;82(2):111–121.

30. Stepanyants A, Hirsch JA, Martinez LM, Kisvárdy ZF, Ferecskó AS, Chklovskii DB. Local potential connectivity in cat primary visual cortex. *Cerebral Cortex*. 2007;18(1):13–28.
31. Kaiser M, Hilgetag CC, Van Ooyen A. A simple rule for axon outgrowth and synaptic competition generates realistic connection lengths and filling fractions. *Cerebral Cortex*. 2009;19(12):3001–3010.
32. Betzel RF, Bassett DS. Specificity and robustness of long-distance connections in weighted, interareal connectomes. *Proceedings of the National Academy of Sciences*. 2018;115(21):E4880–E4889.
33. Laughlin SB, Sejnowski TJ. Communication in neuronal networks. *Science*. 2003;301(5641):1870–1874.
34. Ercsey-Ravasz M, Markov NT, Lamy C, Van Essen DC, Knoblauch K, Toroczkai Z, et al. A predictive network model of cerebral cortical connectivity based on a distance rule. *Neuron*. 2013;80(1):184–197.
35. Karbowski J. Optimal wiring principle and plateaus in the degree of separation for cortical neurons. *Physical review letters*. 2001;86(16):3674.
36. Song HF, Kennedy H, Wang XJ. Spatial embedding of structural similarity in the cerebral cortex. *Proceedings of the National Academy of Sciences*. 2014;111(46):16580–16585.
37. Betzel RF, Avena-Koenigsberger A, Goñi J, He Y, De Reus MA, Griffa A, et al. Generative models of the human connectome. *Neuroimage*. 2016;124:1054–1064.
38. Chen Y, Wang S, Hilgetag CC, Zhou C. Features of spatial and functional segregation and integration of the primate connectome revealed by trade-off between wiring cost and efficiency. *PLoS computational biology*. 2017;13(9):e1005776.
39. Cherniak C. Local optimization of neuron arbors. *Biological cybernetics*. 1992;66(6):503–510.
40. Shannon CE. A mathematical theory of communication. *Bell system technical journal*. 1948;27(3):379–423.
41. Rubinov M, Sporns O. Weight-conserving characterization of complex functional brain networks. *Neuroimage*. 2011;56(4):2068–2079.
42. Braitenberg V, Schüz A. *Cortex: statistics and geometry of neuronal connectivity*. Springer Science & Business Media; 2013.
43. White JG, Southgate E, Thomson JN, Brenner S. The structure of the nervous system of the nematode *Caenorhabditis elegans*. *Philosophical Transactions of the Royal Society of London B, Biological Sciences*. 1986;314(1165):1–340. doi:10.1098/rstb.1986.0056.
44. Chen BL, Hall DH, Chklovskii DB. Wiring optimization can relate neuronal structure and function. *Proceedings of the National Academy of Sciences*. 2006;103(12):4723–4728. doi:10.1073/pnas.0506806103.
45. Chen B. *Neuronal Network of C. elegans: from Anatomy to Behavior*. Cold Spring Harbor Laboratory; 2007.

46. Varshney LR, Chen BL, Paniagua E, Hall DH, Chklovskii DB. Structural properties of the *Caenorhabditis elegans* neuronal network. *PLoS Computational Biology*. 2011;7(2):1–21. doi:10.1371/journal.pcbi.1001066.
47. Achacoso TB YWS. In: *Ay's Neuroanatomy of C. Elegans for Computation*. CRC Press; 1992. p. 79–164.
48. Durbin RM. *Studies On The Development And Organisation Of The Nervous System Of Caenorhabditis Elegans*;
49. Kaiser M, Hilgetag CC. Nonoptimal Component Placement, but Short Processing Paths, due to Long-Distance Projections in Neural Systems. *PLOS Computational Biology*. 2006;2(7):1–11. doi:10.1371/journal.pcbi.0020095.
50. Choe Y McCormick BH KW. Network connectivity analysis on the temporally augmented *C. elegans* web: A pilot study. *Society of Neuroscience Abstracts*. 2004;30(921.9).
51. Chiang AS, Lin CY, Chuang CC, Chang HM, Hsieh CH, Yeh CW, et al. Three-Dimensional Reconstruction of Brain-wide Wiring Networks in *Caenorhabditis elegans* at Single-Cell Resolution. *Current Biology*. 2011;21(1):1–11.
52. Oh SW, Harris JA, Ng L, Winslow B, Cain N, Mihalas S, et al. A mesoscale connectome of the mouse brain. *Nature*. 2014;508:207 EP –.
53. Kötter R. Online retrieval, processing, and visualization of primate connectivity data from the CoCoMac Database. *Neuroinformatics*. 2004;2(2):127–144. doi:10.1385/NI:2:2:127.
54. Carmichael ST, Price JL. Architectonic subdivision of the orbital and medial prefrontal cortex in the macaque monkey. *Journal of Comparative Neurology*. 1994;346(3):366–402. doi:10.1002/cne.903460305.
55. Goldman-Rakic PS, Rakic P. Preface: Cerebral Cortex Has Come of Age. *Cerebral Cortex*. 1991;1(1):1. doi:10.1093/cercor/1.1.1.
56. Lewis JW, Van Essen DC. Mapping of architectonic subdivisions in the macaque monkey, with emphasis on parieto-occipital cortex. *Journal of Comparative Neurology*. 2000;428(1):79–111.
57. Chen Y, Wang S, Hilgetag CC, Zhou C. Trade-off between Multiple Constraints Enables Simultaneous Formation of Modules and Hubs in Neural Systems. *PLOS Computational Biology*. 2013;9(3):1–20. doi:10.1371/journal.pcbi.1002937.
58. Kleitman DJ, Wang DL. Algorithms for constructing graphs and digraphs with given valences and factors. *Discrete Mathematics*. 1973;6(1):79–88.
59. Grant M, Boyd S. CVX: Matlab Software for Disciplined Convex Programming, version 2.1; 2014. <http://cvxr.com/cvx>.
60. Grant M, Boyd S. Graph implementations for nonsmooth convex programs. In: Blondel V, Boyd S, Kimura H, editors. *Recent Advances in Learning and Control. Lecture Notes in Control and Information Sciences*. Springer-Verlag Limited; 2008. p. 95–110.
61. Baruch L, Itzkovitz S, Golan-Mashiach M, Shapiro E, Segal E. Using expression profiles of *Caenorhabditis elegans* neurons to identify genes that mediate synaptic connectivity. *PLoS computational biology*. 2008;4(7):e1000120.

62. Binzegger T, Douglas RJ, Martin KA. A quantitative map of the circuit of cat primary visual cortex. *Journal of Neuroscience*. 2004;24(39):8441–8453.
63. Kolmogorov A. Sulla determinazione empirica di una legge di distribuzione. *G Ist Ital Attuari*. 1933;4:83–91.
64. Smirnov N. Table for Estimating the Goodness of Fit of Empirical Distributions. *The Annals of Mathematical Statistics*. 1948;19(2):279–281.
65. Newman ME. Modularity and community structure in networks. *Proceedings of the national academy of sciences*. 2006;103(23):8577–8582.
66. Newman ME, Moore C, Watts DJ. Mean-field solution of the small-world network model. *Physical Review Letters*. 2000;84(14):3201.
67. Demetrius L, Manke T. Robustness and network evolution—an entropic principle. *Physica A: Statistical Mechanics and its Applications*. 2005;346(3-4):682–696.
68. Izhikevich EM. Polychronization: Computation with Spikes. *Neural Computation*. 2006;18(2):245–282.
69. Honey CJ, Thivierge JP, Sporns O. Can structure predict function in the human brain? *Neuroimage*. 2010;52(3):766–776.
70. Antonopoulos CG, Srivastava S, Pinto SEdS, Baptista MS. Do brain networks evolve by maximizing their information flow capacity? *PLOS computational biology*. 2015;11(8):e1004372.
71. Toker D, Sommer FT. Information integration in large brain networks. *PLoS computational biology*. 2019;15(2):e1006807.
72. Linsker R. Self-organization in a perceptual network. *Computer*. 1988;21(3):105–117.